

Selective leaching of NiAl_3 and Ni_2Al_3 intermetallics to form Raney nickels

M. L. BAKKER, D. J. YOUNG, M. S. WAINWRIGHT

School of Chemical Engineering and Industrial Chemistry, University of New South Wales, P.O. Box 1, Kensington, New South Wales 2033, Australia

Annealed single-phase NiAl_3 and Ni_2Al_3 materials were leached with 20 wt% aqueous NaOH solution to remove the aluminium. At temperatures of 274 to 323 K, NiAl_3 leached according to linear kinetics, yielding porous nickel which was friable and disintegrated. At these temperatures Ni_2Al_3 was unreactive, but at 343 to 380 K it leached according to parabolic kinetics, producing a strong, tightly adherent rim of residual material. The Ni_2Al_3 reaction proceeded in two steps, firstly to produce a two-phase mixture of Ni_2Al_3 plus nickel, and secondly to produce nickel alone. In both stages the detailed microstructure of the prior alloy was preserved, implying that the mechanism is selective dissolution. The surface adsorption properties of the nickel residues were obscured by reprecipitated alumina. However, metal crystallite size measurements showed that a large nickel surface area was potentially available.

1. Introduction

It has long been known [1, 2] that alkaline dissolution of aluminium from Ni-Al alloys leaves a porous, high surface-area nickel residue. This residue is known as Raney nickel and is widely used as a catalyst for liquid-phase hydrogenation reactions. The material is very friable and is used in slurry form. In this form, the material cannot be used in gas-phase reactions, where its catalytic activity might otherwise make it attractive. There is thus some practical interest in producing Raney nickel in a strong, aggregated form.

The process whereby aluminium leaching from Ni-Al alloys occurs is rather poorly understood. Because the morphology, and hence the surface properties, of the resultant material, will obviously be determined by this process, there exists a need to define the nature of the reaction.

The commercial alloys from which Raney nickel is produced are usually 50 wt% Ni-50 wt% Al. These alloys have quenched structures and therefore consist of the intermetallics Ni_2Al_3 and NiAl_3 as well as some frozen eutectic. It is known [3-10] that the eutectic material leaches more rapidly than NiAl_3 which leaches much more rapidly than Ni_2Al_3 . If the reaction is carried far enough, essentially all of the aluminium is removed from the alloy [3], although quite large amounts of hydrated alumina are re-precipitated from the aqueous phase [5-7, 9, 11].

There appears to be no knowledge of the contributions made by each of NiAl_3 and Ni_2Al_3 to the properties of the residue obtained from the two-phase alloy. Because the volume fractions of nickel in these two intermetallics are obviously different, a difference in the pore morphologies of the leach products might be expected. Many examinations have been made [5-7, 10] of the effect of variations in leach reaction conditions on catalyst properties. The results

do not form a self-consistent whole, quite probably because the different nickel aluminides respond differently to alterations in reaction conditions. On the other hand, the leaching behaviour of a single-phase CuAl_2 material has been shown [12-15] to be quantitatively described in terms of classical phase transformation theory.

The aims of this work were accordingly to study the leaching behaviour of single-phase NiAl_3 and Ni_2Al_3 materials and to determine the morphologies of their leach residues. A subsidiary aim was to see if any possibility existed of producing a strong, cohesive Raney nickel in a simple leaching process.

2. Experimental details

The starting materials used were Ni-Al alloy provided by the Davison Division, W. R. Grace Co. (Baltimore, Maryland, USA). Chemical analysis by atomic absorption spectrophotometry showed that the two alloys contained 57.5 and 39.8 wt% Al, corresponding, respectively, to NiAl_3 with a slight excess of nickel, and to Ni_2Al_3 . Each alloy was re-melted in an argon arc furnace using non-consumable electrodes, and cast into small rod-shaped ingots. These were subsequently annealed for 24 h under flowing hydrogen at a temperature of 1103 K for NiAl_3 and 1363 K for Ni_2Al_3 . These temperatures are slightly below the peritectic decomposition points of the respective phases. Subsequent X-ray diffraction and metallographic examination confirmed that the Ni_2Al_3 material was single-phase whereas the NiAl_3 material contained a small concentration of Ni_2Al_3 inclusions. The annealed materials were cut into approximately cubic pieces of ~4 mm, the surfaces of which were metallographically polished to 1 μm finish.

Alloy pieces were reacted with a very large excess of 20 wt% aqueous NaOH solution. Reaction

temperatures of 274, 293 and 323 K were used for NiAl₃ and 343, 363 and 380 K for Ni₂Al₃. Individual pieces were removed from the leach solution at various time intervals, and washed in water to quench the reaction. Metallographic cross-sections of these samples revealed a reaction-affected rim, the thickness of which was measured with an optical microscope using a vernier eyepiece.

The material in the reaction-affected rim was identified by X-ray diffraction, and by electron probe microanalysis in which the results of point counting relative to elemental standards were corrected for atomic number, absorption and fluorescence effects. Because the rims were porous, the concentrations calculated from the correction procedure totalled less than 100%. The values were scaled up accordingly. The morphology of the product material was characterized with respect to pore volume, surface area and crystallite size. Pore volumes and surface areas were measured by gas uptake using a flow adsorption/desorption method [16]. Crystallite sizes were determined from X-ray line broadening corrected for instrumental effects using a KCl standard.

Because the leach residue was pyrophoric it was stored under de-aerated water. Vacuum impregnation with epoxy resin, used in preparing metallographic samples, served to protect the material from oxidation. Freshly prepared material was coated with collodion prior to X-ray analysis.

3. Results

3.1. Reaction morphology

Both alloys leached to form a rim of reaction-affected material. The rim formed on NiAl₃ was initially reasonably coherent, but tended to disintegrate once its thickness exceeded about 200 μm. The appearance of these rims is shown in Fig. 1 where the sharply defined interface between reaction product and as-yet unattacked alloy is evident. In the case of Ni₂Al₃, the reaction-affected rims were always coherent and strongly adherent to the unreacted alloy core. As shown in Fig. 2, the rim formed at 363 K consisted of a single layer; at 380 K the rim was initially the same, but when the leaching depth became very large, a second layer was formed in the outer part of the rim. Whereas the outer layer was apparently featureless,

the first-formed, inner layer had a well-developed microstructure. This is seen in Fig. 3 to be a two-phase structure. Scanning electron microscopic examination of the prior alloy produced a weak contrast image which appeared to show a similar structure. Apart from local incursions along cracks, the interface between alloy and rim was planar (i.e. parallel to the external surface) and sharply defined. The interface between inner and outer sublayers was also planar, although somewhat less well defined.

3.2. Reaction kinetics

The increase in leach depth, X , with time is shown for the intermetallics in Figs 4 and 5. In the case of NiAl₃, because the reaction product tended to disintegrate after some extent of reaction, it was not possible to measure rim thicknesses. Instead the recession of the alloy surface is reported. The kinetics are seen to be rapid and approximately linear at 293 and 323 K, but a diminution in rate with increasing extent of reaction is evident at 274 K.

Kinetics for the leaching of Ni₂Al₃ are plotted in Fig. 5 according to the parabolic rate equation

$$X + X' = (k_p t)^{1/2} \quad (1)$$

where X is the thickness of product layer produced in time, t , and where X' , k_p are constants. This relationship is seen to provide a good description of the data apart from the early stages of reaction at the higher temperatures. No leaching at all was found at lower temperatures, and even at the higher temperature employed, very slow kinetics were observed.

3.3. Reaction product characterization

Analysis by X-ray diffraction of the leached rim formed on NiAl₃ revealed the presence of microcrystalline nickel, some Ni₂Al₃ and hydrated alumina (in the form of gibbsite). In addition, a small amount of NiO was detected in the material leached at 323 K. Leach residues removed from partially leached Ni₂Al₃ contained both microcrystalline nickel and Ni₂Al₃. However, after leaching to completion, the residue was identified by X-ray diffraction as consisting of microcrystalline nickel only. No crystalline forms of hydrated alumina were detected at any stage of leaching. The results of electron probe microanalysis of

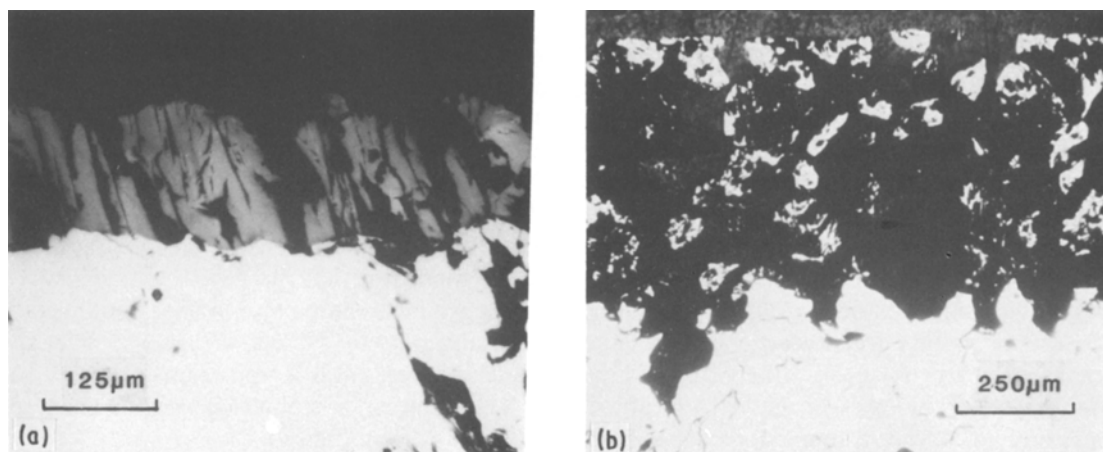


Figure 1 Cross-sections of reaction product rims formed on NiAl₃ (a) after leaching for 1.3 h at 293 K, (b) after leaching for 10 h at 293 K.

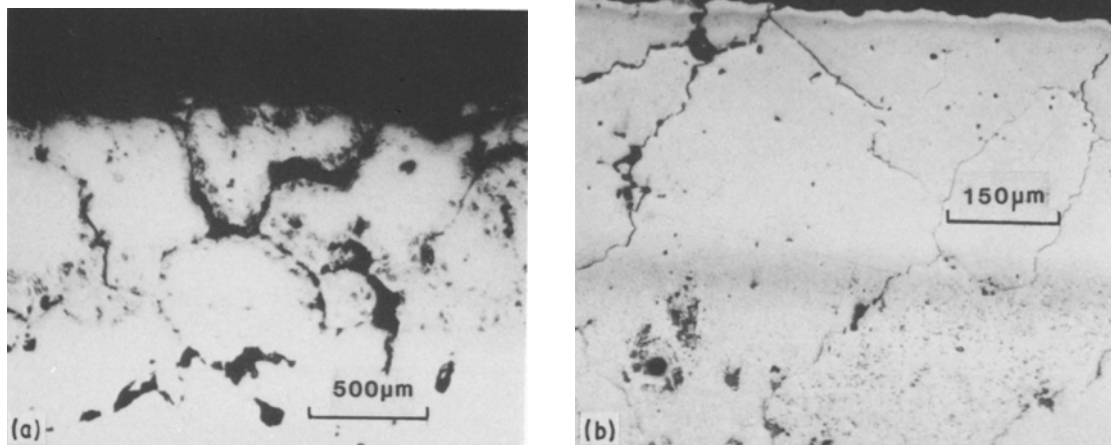


Figure 2 Cross-sections of reaction product rims formed on Ni_2Al_3 (a) after leaching for 200 h at 363 K, (b) after leaching for 200 h at 380 K.

cross-sections of partially and completely leached Ni_2Al_3 pieces are shown in Fig. 6.

Surface areas and pore volumes measured by gas uptake on samples leached for various times are shown for NiAl_3 and Ni_2Al_3 in Tables I and II, respectively. In the case of NiAl_3 , the leach residue was removed from the substrate alloy prior to the adsorption measurement. This procedure was not practicable for Ni_2Al_3 as the residue material was too strong. Instead the composite piece was used in its entirety, and gas uptake measurements corrected for the presence of a non-adsorbing alloy core. Nickel crystallite sizes measured by X-ray line broadening are also shown in these tables.

4. Discussion

Leaching of both NiAl_3 and Ni_2Al_3 leads, ultimately, to the formation of highly porous nickel. In both cases a sharp interface is formed between as-yet unaffected alloy and the nickel residue. Such a pattern of behaviour could result from the simultaneous dissolution of both metals followed by the reprecipitation of the

more noble nickel [4, 9]. It could also occur as a result of selective dissolution of the aluminium, leaving a nickel skeleton [5–8]. The latter view is suggested by the low solubility of nickel in alkali solution. It is supported by the finding that prior alloy microstructures are preserved in the leach residue when composite alloys, containing both NiAl_3 and Ni_2Al_3 , are subjected to alkali extraction. However, those earlier experiments involved rather short reaction times, and it is not clear that the deduction of a selective dissolution mechanism applies to the leaching of Ni_2Al_3 . The question is of interest because a quantitative theory of selective dissolution is available [12, 15] for the prediction of product morphologies.

A striking difference in reactivity of the two nickel aluminate phases is evident in the present results, and has been noted before in qualitative terms, [4, 6–10]. The present findings permit a rather more precise statement of this difference, in terms of the reaction kinetics and morphology.

Leaching of NiAl_3 proceeds according to rapid linear kinetics at temperatures of 293 and 323 K, associated with the formation of a reaction product which lacks coherency and largely disintegrates after a relatively small extent of reaction. Clearly, then, the accumulation of reaction product plays little part in controlling the leaching process which accordingly proceeds

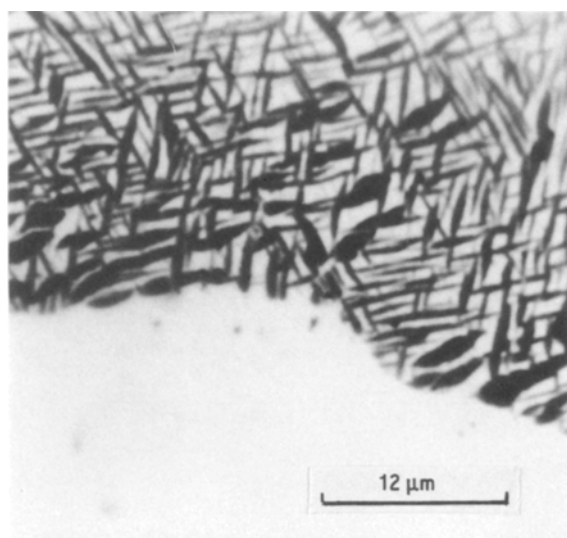


Figure 3 Enlarged view of interface between Ni_2Al_3 and inner reaction product rim (sample leached for 200 h at 380 K).

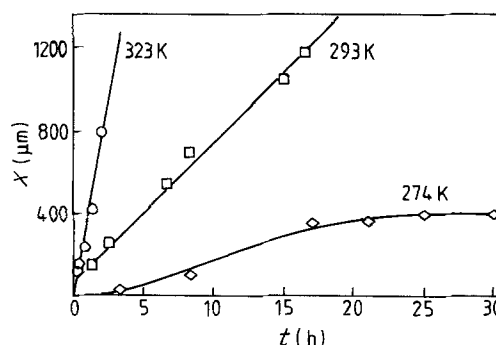


Figure 4 Leaching kinetics for NiAl_3 as measured by alloy surface recession.

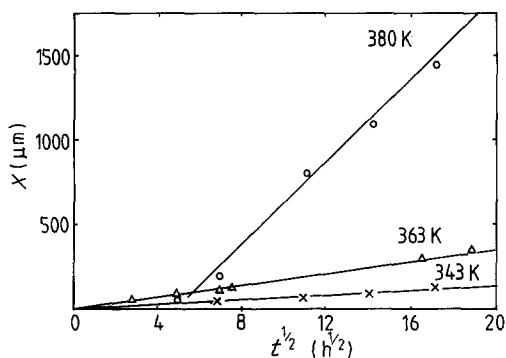


Figure 5 Leaching kinetics for Ni_2Al_3 as measured from thickness of product layer. Straight lines represent regression on parabolic rate equation.

at an unvarying rate. At a temperature of 274 K, the rate does slow with increasing extent of reaction.

The volume fraction of nickel in the leach residue may be calculated from the known densities of NiAl_3 and nickel as having the value 0.19. This calculation assumes no shrinkage of the rim, an assumption which appears unlikely to be valid in view of the cracks apparent in the residue material (Fig. 1a). Nonetheless, a large void fraction is to be expected, and the fact that the product is very weak and friable is, therefore, explicable. Its failure to form a protective layer on the alloy surface presumably results from the destruction of the weak material by the hydrogen evolution which accompanies the reaction. The protective effect found at 274 K may be due to partial persistence of the nickel layer when gas evolution is slow. It is concluded that the formation of significant quantities of coherent Raney nickel from NiAl_3 is not possible.

In addition to nickel, the leach residue from NiAl_3 contained some Ni_2Al_3 as well as NiO and hydrated Al_2O_3 . The Ni_2Al_3 is simply remnant material from the original alloy, as the reaction conditions were too mild to induce attack on this phase. The presence of alumina has been noted before [5, 7, 9, 11] and results from precipitation from the liquid phase.

Leaching of Ni_2Al_3 proceeded at observable rates only at temperatures of 343 K and above. Slow parabolic kinetics were associated with the formation of a strongly coherent and adherent reaction product layer. The volume fraction of nickel in completely leached Ni_2Al_3 is calculated from the densities of Ni_2Al_3 and nickel as 0.40. This relatively high value

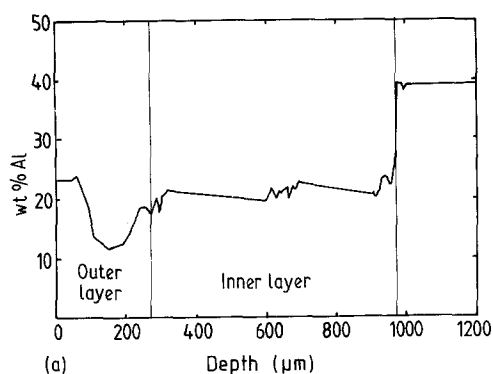


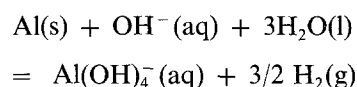
TABLE I Surface properties of NiAl_3 residues

Extraction temp. (K)	Extraction time (h)	Surface area ($\text{m}^2 \text{g}^{-1}$)	Pore volume ($\text{cm}^3 \text{g}^{-1}$)	Crystal size (nm)
274	7.0	16	0.122	38
	9.5	10	0.122	60
	16.2	8	0.073	52
	20.0	8	0.053	42
293	2.0	38	0.034	7
	5.0	43	0.036	6
	7.9	46	0.102	11
	13.8	52	0.065	7
	16.6	53	0.084	9
323	0.6	30	0.039	9
	1.1	56	0.065	7
	1.7	63	0.085	7
	2.2	58	0.077	8

presumably accounts for the strength of the product material.

The observation of parabolic kinetics suggests that the reaction is controlled by diffusion through the product layer. Obviously solid-state diffusion across the width of this layer would be far too slow to support the observed reaction rates, and we consider instead diffusion through the liquid which occupies the layer's pore space.

From the stoichiometry of the reaction



it is apparent that the material fluxes, J , through the product rim, are related according to

$$J_{\text{Al}} = -J_{\text{OH}^-} \quad (2)$$

The value of J_{OH^-} can be evaluated by approximating Fick's first law as

$$J_{\text{OH}^-} = -\frac{D(C - C_0)}{X} \quad (3)$$

where C is the hydroxyl concentration in the bulk liquid and C_0 its value at the alloy-product layer interface. The aluminium flux is found from the mass balance at this interface using Equation 1.

$$J_{\text{Al}} = \frac{1}{V_{\text{Al}}} \frac{k_p}{2(X + X')} \quad (4)$$

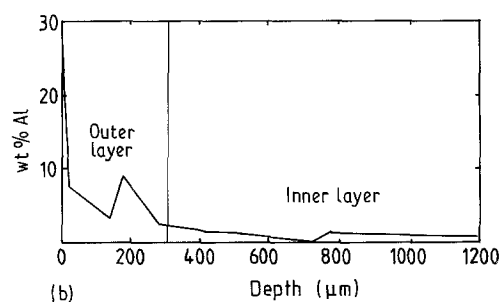


Figure 6 Electron probe microanalysis of product rims formed on Ni_2Al_3 (a) after leaching for 200 h at 380 K, (b) after leaching to completion (300 h at 380 K).

TABLE II Surface properties of Ni₂Al₃ residues

Extraction temp. (K)	Extraction time (h)	Surface area (m ² g ⁻¹)	Pore volume (cm ³ g ⁻¹)	Crystal size (nm)
343	196	6	0.128	104
	455	12	0.066	32
	558	21	0.026	10
	676	14	0.042	20
363	48	101	0.326	13
	74	88	0.192	11
	147	97	0.125	17
	221	10	0.012	15
	272	23	0.025	11
380	48	84	0.252	13
	97	35	0.066	11
	144	22	0.065	17
	196	17	0.034	15
	293	23	0.031	11

where V_{Al} is the molar volume of aluminium in the alloy. Combination of Equations 2, 3 and 4, using the approximations $X' \approx 0 \approx C_o$, then yields

$$D_{OH^-} \approx k_p/2CV_{Al} \quad (5)$$

Application of Equation 5 to the rate data reported in Fig. 5 leads to estimates for D_{OH^-} of 1×10^{-9} , 1×10^{-8} and 1×10^{-6} cm² sec⁻¹ at 343, 363 and 380 K, respectively. These values are considerably lower than those expected for diffusion of aqueous hydroxide ions. The data of Fig. 5 can also be used to arrive at an estimate of the Arrhenius activation energy for reaction. In this way a value of 110 kJ is found, quite inconsistent with normal liquid-phase diffusion. It is concluded, therefore, that liquid-phase diffusion of hydroxyl ions is fast enough to support the observed reaction rates, but does not control them. The nature of the rate-determining process is not revealed by the present experiments.

The reaction product layer produced on Ni₂Al₃ was considerably more complex than that found on NiAl₃. Reaction apparently proceeded in two stages, producing two distinct layers of material when the extent of reaction was large. As the reaction neared completion, that is to say, as the central alloy core was exhausted, the compositions of both layers changed.

Examination of the concentration profile for a partially leached sample of Ni₂Al₃ in Fig. 6a reveals a discontinuous change in composition at the alloy-product interface. This finding, together with the absence of any depletion within the alloy, is consistent with a mechanism of selective dissolution. The inner layer of the product rim has an approximately uniform composition of about 22 wt % Al. There exists no single Ni-Al phase of this composition, although the phase NiAl, containing 24 to 37 wt % Al is reasonably close. In the outer layer, the aluminium content reaches a minimum of about 12 wt % Al and then rises to a maximum of around 24 wt % at the external surface. Again, no single Ni-Al phase exists with an aluminium content of 12 wt % Al. Evidently the two sublayers of the rim each contain more than one phase. This deduction is confirmed in the case of the inner layer by its visible microstructure, as shown in Fig. 3.

X-ray diffraction of the leached material revealed

the presence of nickel and Ni₂Al₃ only. In addition, the possible presence of amorphous Al₂O₃ · xH₂O must be recognized [5, 6]. Microprobe analysis of a sample approaching complete leaching (Fig. 6b) showed that the aluminium content of the inner layer approaches zero, whilst that of the outer layer is somewhat reduced but still has a high value at the rim surface. Consistent with all of these observations, it is concluded that partial leaching of Ni₂Al₃ leads to the formation of a composite residue consisting of Ni₂Al₃ plus nickel. The outer part of the leached rim is more extensively reacted, producing a higher Ni/Ni₂Al₃ ratio. However, reprecipitation of an alumina hydrate near the rim exterior leads to an increase in aluminium content, as measured with the microprobe. It is further concluded that prolonged leaching leads to reaction of the remnant Ni₂Al₃ material leaving only nickel and reprecipitated alumina present.

A reaction which converts Ni₂Al₃ into a mixture of Ni₂Al₃ plus nickel whilst preserving the detailed microstructure of the parent alloy is obviously one of selective dissolution. What is not yet clear is why some of the original Ni₂Al₃ is more readily leachable than the rest. The reason is presumably connected with the detailed microstructure of the precursor intermetallic, as reflected in the reaction product (Fig. 3). Unfortunately, the scale of this structure is too fine for conventional microanalysis.

The surface properties of both NiAl₃ and Ni₂Al₃ leach residues are unfortunately obscured by the reprecipitated alumina. Theoretical pore volumes for fully leached NiAl₃ and Ni₂Al₃ are, respectively, 0.48 and 0.17 cm³ g⁻¹. Reference to Tables I and II shows that for Ni₂Al₃ short leaching times sometimes produce pore volumes in excess of those theoretically possible. At long times, when leaching is essentially complete, both phases exhibit apparent pore volumes very much less than those expected. It is concluded, therefore, that what is being measured by gas adsorption is not characteristic of the metal but reflects rather the properties of the alumina. Similar findings have been reported [6, 7, 9] for conventional Raney nickel materials.

Metal crystallite sizes measured from X-ray line broadening are reliable, however, and indicate that large metal surface areas are potentially available. In calculating the possible size of these areas from the crystallite dimensions, it is necessary to know the detailed geometry of the residue. The necessary information is lacking for nickel, but has been reported for copper residues prepared by selectively leaching CuAl₂. In this latter case the metal consists of single-crystal fibres of circular cross-section oriented approximately parallel to the direction of the leaching reaction [14]. If the same morphology is adopted by the nickel residue, then surface areas of about 45 to 55 m² g⁻¹ are calculated for nickel particles of size ranging from 10 down to 8 nm. Because the volume fraction of nickel in the residue formed from Ni₂Al₃ is so much higher than that of copper formed from CuAl₂ (0.40 compared with 0.25), it may be that a morphology consisting of pores through a continuous metal matrix is favoured. Surface areas calculated for such a

morphology are very similar to those found for the earlier case. It is tentatively concluded on this basis that the Ni_2Al_3 leach residue may well have a high metal surface area but that it has not yet been measured because of fouling by reprecipitated alumina.

5. Conclusions

It has been demonstrated that the leaching of NiAl_3 leads to the formation of nickel residue which lacks strength and tends to disintegrate. On the other hand, the residue formed from Ni_2Al_3 is strong and remains attached to the substrate material. This difference in behaviour is attributed to the difference in void volume fractions calculated for the two materials.

Leaching kinetics were approximately linear for NiAl_3 as a result of the failure of the residue to form a protective layer. For Ni_2Al_3 the kinetics were parabolic. Although hydroxide ion diffusion within the liquid-filled pore space of the product layer is rapid enough to support the observed rates, it seems unlikely to be the rate-controlling process.

The mechanism whereby Ni_2Al_3 leaches was found to be selective dissolution rather than dissolution-reprecipitation. This conclusion is based firstly on the fact that the prior alloy microstructure is preserved in the product layer and, secondly, on the observation that the alloy leaches initially to provide a two-phase mixture of nickel plus Ni_2Al_3 , and finally to leave only nickel.

Reprecipitation of alumina interfered with surface adsorption measurements. However, the nickel metal was found to be very finely microcrystalline, and a large surface area is potentially available.

References

1. M. RANEY, US Patent, 1 563 787 (1925).
2. *Idem, ibid.* 1 628 191 (1926).
3. R. SASSOULAS and Y. TRAMBOUZE, *Bull. Soc. Chim. Fr.* **5** (1964) 985.
4. A. A. PRESNYAKOV, K. T. CHERNOUSOV, T. KABIEV, A. B. FASMAN and T. T. BOCHAROVA, *Zh. Prikl. Khim.* **40** (1967) 958.
5. J. FREEL, W. J. M. PIETERS and R. B. ANDERSON, *J. Catal.* **14** (1969) 247.
6. *Idem, ibid.* **16** (1970) 281.
7. S. D. ROBERTSON and R. B. ANDERSON *ibid.* **41** (1976) 405.
8. D. J. YOUNG, M. S. WAINWRIGHT and R. B. ANDERSON, *ibid.* **64** (1980) 116.
9. V. R. CHOUDHARY and S. K. CHOUDHARI, *J. Chem. Tech. Biotech.* **33A** (1983) 330.
10. S. SANE, J. M. BONNIER, J. P. DAMON and J. MASSON, *Appl. Catal.* **9** (1984) 69.
11. F. DELANNAY, J. P. DAMON, J. MASSON and B. DELMON, *ibid.* **4** (1982) 169.
12. A. D. TOMSETT, D. J. YOUNG and M. S. WAINWRIGHT, *J. Electrochem. Soc.* **131** (1984) 2476.
13. N. I. ONOUHA, A. D. TOMSETT, M. S. WAINWRIGHT and D. J. YOUNG, *J. Catal.* **91** (1985) 25.
14. J. SZOT, D. J. YOUNG, A. BOURDILLON and K. E. EASTERLING, *Phil. Mag. Lett.* **55** (1987) 109.
15. A. D. TOMSETT, D. J. YOUNG and M. S. WAINWRIGHT, *J. Electrochem. Soc.*, unpublished results.
16. F. M. NELSON and F. T. EGGERTSEN, *Anal. Chem.* **30** (1958) 1387.

*Received 23 July
and accepted 23 October 1987*